

Sol–Gel Prepared Sn–Al_2O_3 Catalysts for the Selective Reduction of NO with Propene

Masaaki Haneda,* Shin-ichi Ohzu,† Yoshiaki Kintaichi, Ken-ichi Shimizu,†† Junji Shibata,††† Hisao Yoshida,††† and Hideaki Hamada

National Institute of Advanced Industrial Science and Technology(AIST), AIST Tsukuba Central 5, 1-1-1 Higashi, Tsukuba, Ibaraki 305-8565

†Faculty of Science and Technology, Science University of Tokyo, 2641 Yamazaki, Noda, Chiba 278-8510

††Graduate School of Science and Technology, Niigata University, Ikarashi, Niigata 950-2181

†††Graduate School of Engineering, Nagoya University, Chikusa-ku, Nagoya 464-8603

(Received April 19, 2001)

Catalytic reduction of NO by propene in the presence of oxygen was studied over Sn–Al_2O_3 prepared by the sol–gel method. The maximum NO conversion did not change much with Sn loading (1–5 wt%), although the effective temperature window for NO reduction shifted to lower temperatures with increasing Sn loading. X-ray diffraction (XRD), and X-ray absorption spectroscopy (XANES and EXAFS) revealed the formation of finely-divided SnO_2 crystallites in Sn–Al_2O_3. It was deduced that not only the surface vicinity of supported SnO_2, which can be reduced at lower temperatures, but also alumina participate in the reaction as catalytically active sites. The catalytic performance of Sn–Al_2O_3 was markedly improved by an H_2O treatment at 873 K. The H_2O treatment did not affect the crystal structure of the catalysts and the dispersion state of supported SnO_2, but promoted the removal of Cl^- ions, which originated from the $SnCl_4$ precursor. The activity enhancement by the H_2O treatment was accounted for by an increase in the surface SnO_2 concentration as active sites and by the modification of oxo-tin species as active sites. Reaction kinetic studies suggested that NO reduction on the fresh and the H_2O-treated catalysts proceeds through the same reaction pathway in which the surface NO_x adspecies and C_3H_6-derived species play an important role for NO reduction.

Selective catalytic reduction of nitrogen oxides (NO_x) in the presence of oxygen is a challenging subject of study.[1] Since the first reports of NO reduction by hydrocarbons over Cu–ZSM-5 by Iwamoto et al.[2] and by Held et al.[3] following patent literature,[4,5] many investigations have focused on zeolite-based catalysts.[6–8] Although metal ion-exchanged zeolites showed excellent activity at high space velocities, their deactivation under hydrothermal conditions due to dealumination from the framework is a serious problem from a practical viewpoint.[9]

In addition to zeolite-based catalysts, metal oxide-based catalysts have also been found to catalyze this reaction.[10,11] Concerning single metal oxides, we first reported the catalytic performance of solid acid or base-type oxides, such as Al_2O_3, ZrO_2 and MgO.[12] Teraoka et al.[13] also reported that SnO_2 showed good activity for NO reduction by hydrocarbons under the reaction conditions of low space velocities and relatively low O_2/hydrocarbon ratios. Generally, metal oxides can be characterized by high selectivity and stability, although their activity is relatively low compared with zeolites. Therefore, many studies have tried to enhance their catalytic activity.

The catalytic performance of metal (oxide) is often promoted by supporting it onto high surface area support. Tabata et al.[14] and Kung et al.[15,16] reported that the catalytic activity of Al_2O_3 for NO reduction by methanol and propene was considerably enhanced at low temperatures by the addition of SnO_2. Ma et al.[17] also reported that SnO_2–ZrO_2 binary oxides showed good activity for NO reduction by propene. Such a positive effect of support would be accounted for by improved dispersion of SnO_2 induced by a strong interaction with the support.[18]

In the present work, we investigated the catalytic performance of Sn–Al_2O_3 catalysts prepared by the sol–gel method, which is a useful method to prepare catalysts with highly dispersed species,[19,20] for the selective reduction of NO with propene. Several characterizations as well as kinetic studies were also made to probe the properties of supported tin species.

Experimental

1. Catalyst Preparation. Alumina and alumina-supported tin oxide catalysts were prepared by the sol–gel method. The aluminium boehmite sol was first prepared by the hydrolysis of aluminium(Ⅲ) triisopropoxide in hot water (363 K) with a small amount of nitric acid. Then, a solution of tin(IV) chloride dissolved in ethylene glycol was added into the aluminium boehmite sol solution. In the case of Al_2O_3 alone, this procedure was excluded. After the sol solution was stirred at room temperature for 1 day, the solvents were removed by heating under reduced pressure, followed by drying at 383 K in an oven and calcination at 873 K for 5 h in flowing air. The catalyst samples including tin oxides are abbreviated as Sn(x)–Al_2O_3, where "x" is the loading of tin changing from 1 to 10 wt% as Sn. Pure SnO and SnO_2 pow-

ders were purchased from Wako Pure Chemical Industries.

2. Catalytic Reaction. (a) Activity Measurements. The catalytic activity was measured by using a fixed-bed flow reactor. A feed gas mixture containing 880 ppm NO, 950 ppm C_3H_6, 9.3% oxygen and 0 or 9.1% H_2O diluted in helium as a balance gas was fed to 0.2 g of a catalyst at a rate of 66 cm^3 min^{-1} (W/F = 0.18 gs cm^{-3}). H_2O was introduced into the reaction gas mixture with a micro pump. In this case, the feed-gas flow rate and the concentrations of the other gas components were fixed by controlling the helium flow rate. The reaction temperature was changed from 873 to 523 K with steps of 50 K. The analysis of the effluent gas was made with two gas chromatographs equipped with a Molecular Sieve 5A column (for the analysis of N_2 and CO) and a Porapak Q column (for that of N_2O, CO_2 and C_3H_6). The catalytic activity was evaluated in terms of NO conversion to N_2 and that of propene to CO_x (CO + CO_2). The formation of N_2O was found to be negligible in the present study.

(b) Kinetic Studies. The reaction rate of N_2 and CO_x formation was evaluated by changing the catalyst weight from 0.03 to 0.1 g to obtain a conversion level of NO below 30%. The kinetic parameters were determined at 623 K by changing the concentrations of the reactants in the range of 180–1500 ppm for NO, 150–1900 ppm for C_3H_6 and 2–15% for O_2. The total flow rate was 66 cm^3 min^{-1}. The standard reaction gas contained 880 ppm NO, 950 ppm C_3H_6 and 9.3% O_2. The activation energy was calculated at temperatures ranging from 623 to 723 K for the standard reaction gas.

3. Catalyst Characterization. The BET surface area of the catalysts was determined with a conventional flow apparatus (Micromeritics Flowsorb II) by nitrogen adsorption at 77 K. Elemental analysis was conducted by the inductively coupled plasma (ICP) method using a Shimadzu ICP-2000. The crystal structure of the catalysts was identified by X-ray diffraction (XRD) measurements with a Mac Science M18XHF[22] using Cu $K\alpha$ radiation at 40 kV and 74 mA. The local structures around Sn ions were studied by measuring the Sn K-edge X-ray absorption spectra at BL-10B of the Photon Factory in High-Energy Accelerator Research Organization with a ring energy of 2.5 GeV and a stored current of 250–350 mA. The spectra were recorded in a transmission mode at room temperature with a Si(311) channel cut monochromator.

Temperature-programmed reduction (TPR) measurements were carried out in the same manner as described elsewhere.[21] After 0.05 g of a catalyst was pretreated in flowing air at 873 K for 1 h prior to TPR measurements, a 10 vol% H_2–Ar gas mixture was used as a reducing gas with a flow rate of 30 cm^3 min^{-1}; the temperature of the catalyst bed was raised at a heating rate of 5 K min^{-1}. Reduction of CuO to metallic copper was used to calibrate the TPR apparatus for H_2 consumption.

Results and Discussion

1. Catalytic Activity of Sn–Al_2O_3. Figure 1 shows the catalytic activity of Sn–Al_2O_3 with different Sn loadings for NO reduction by propene in the absence of H_2O, along with that of Al_2O_3 and SnO_2. Al_2O_3 effectively catalyzed this reaction at temperatures of around 773–873 K. SnO_2 also served as a catalyst for this reaction at lower temperatures. Obviously, the addition of tin oxide into Al_2O_3 by the sol–gel method caused a considerable enhancement of NO conversion, although no great difference in C_3H_6 conversion between SnO_2 and Sn–Al_2O_3 was observed. It was also found that the effective temperatures for NO reduction on Sn–Al_2O_3 were almost the same as those on SnO_2. These results suggest that the supported tin oxide plays an important role as catalytically active sites.

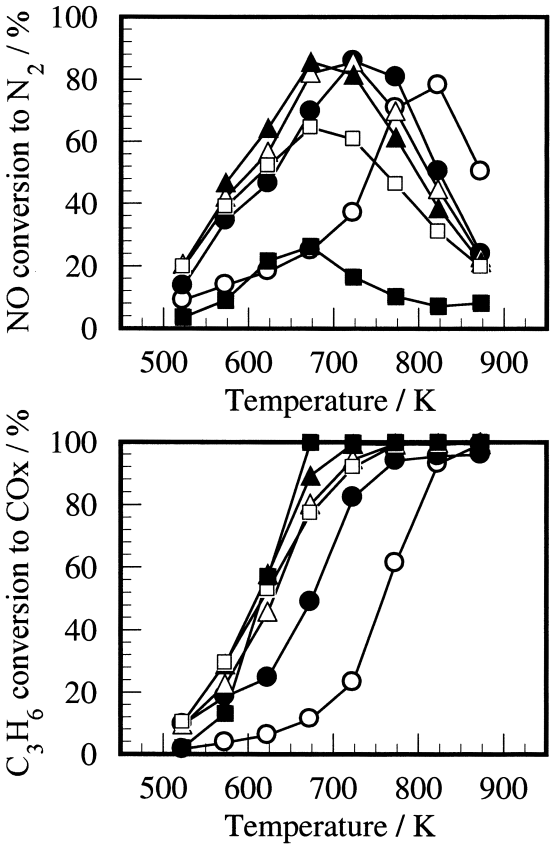

Fig. 1. Effect of Sn loading on the catalytic activity of Sn–Al_2O_3 for NO reduction by propene in the absence of H_2O. Conditions: NO = 880 ppm, C_3H_6 = 950 ppm, O_2 = 9.3%, H_2O = 0%, W/F = 0.18 gs cm^{-3}. (○) Al_2O_3, (●) Sn(1)–Al_2O_3, (△) Sn(3)–Al_2O_3, (▲) Sn(5)–Al_2O_3, (□) Sn(10)–Al_2O_3, (■) SnO_2.

Figure 2 shows the effect of H_2O on the activity of Sn–Al_2O_3. Coexisting H_2O caused a considerable decrease in the activity of Al_2O_3 and SnO_2. On the other hand, Sn–Al_2O_3 still showed relatively high catalytic activity even in the presence of H_2O. No great change in the maximum NO conversion by coexisting H_2O was observed. However, the effective temperature window shifted to 50–100 K in the higher temperature region. It is noteworthy that Sn(3)–Al_2O_3 and Sn(5)–Al_2O_3 showed very similar catalytic performance irrespective of H_2O. The optimum Sn loading seems to be 1–5 wt%.

2. Structural Analysis Table 1 summarizes the physical properties of the catalysts used in this study. The BET surface area of Sn–Al_2O_3 increased along with an increase in Sn loading up to 10 wt%. Elemental analysis revealed that the loading of Sn is close to the calculated value. It should be pointed out that certain amount of Cl^- ions, originating from $SnCl_4$ as the tin precursor, remains even after calcination at 873 K. Figure 3 shows XRD patterns of Sn–Al_2O_3 with different Sn loadings. No diffraction peaks assigned to tin compounds were detected for all of the Sn–Al_2O_3 samples. In addition, a shift in the

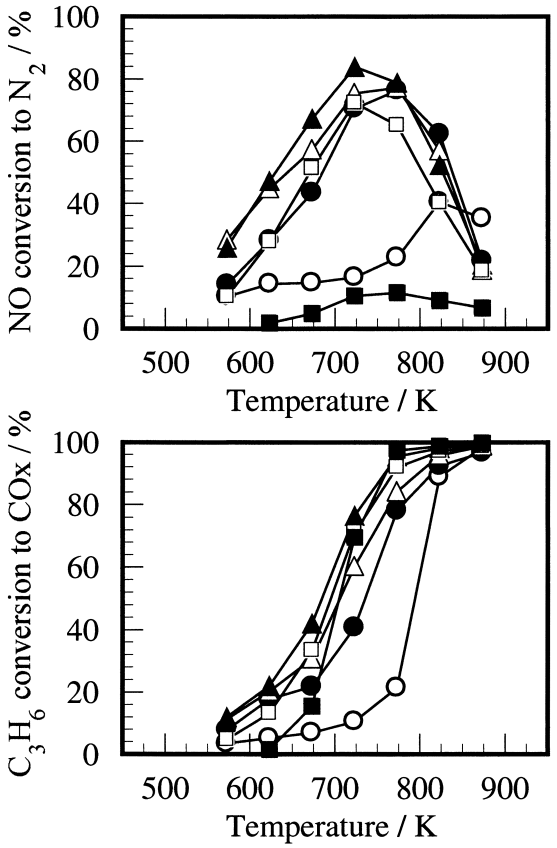

Fig. 2. Effect of H_2O on the catalytic activity of Sn–Al_2O_3 with different Sn loading for NO reduction by propene. Conditions: NO = 880 ppm, C_3H_6 = 950 ppm, O_2 = 9.3%, H_2O = 9.1%, W/F = 0.18 gs cm^{-3}. (○) Al_2O_3, (●) Sn(1)–Al_2O_3, (△) Sn(3)–Al_2O_3, (▲) Sn(5)–Al_2O_3, (□) Sn(10)–Al_2O_3, (■) SnO_2.

Table 1. Physical Properties of the Catalysts Prepared

Catalyst	BET surface area/m^2 g^{-1}	Elemental analysis	
		Sn/Al[a)]	Cl/Al
Al_2O_3	167	na	na
SnO	20	na	na
SnO_2	25	na	na
Sn(1)–Al_2O_3	205	na	na
Sn(3)–Al_2O_3	236	0.014 (0.013)	0.011
Sn(5)–Al_2O_3	231	0.020 (0.023)	0.011
Sn(10)–Al_2O_3	267	0.048 (0.048)	0.020

na: not available.
a) In parentheses are given calculated atomic ratio.

XRD peaks ascribed to γ-Al_2O_3 was not recognized. These results suggest the presence of highly dispersed tin species on Al_2O_3.

In order to obtain information on the local structures around Sn ions, X-ray absorption measurements were performed. Figure 4A shows Sn K-edge XANES (X-ray absorption near edge structures) spectra of Sn–Al_2O_3 together with that of pure SnO and SnO_2 as reference samples. The XANES spectra of Sn–Al_2O_3 were very similar to that of SnO_2, indicating that Sn is present in the +4 oxidation state irrespective of Sn loading.

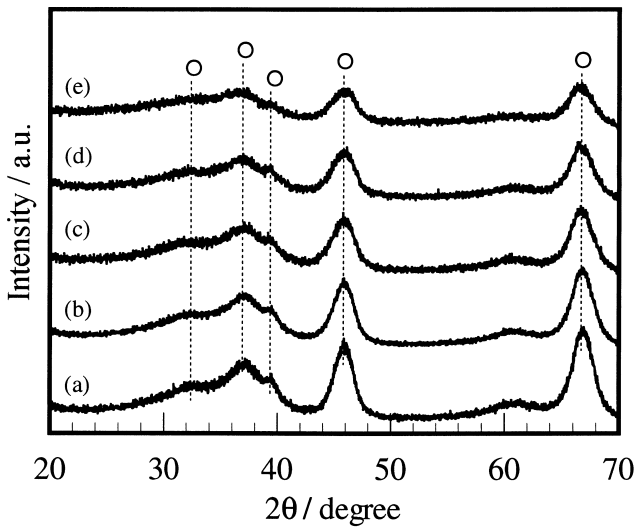

Fig. 3. XRD patterns of (a) Al_2O_3, (b) Sn(1)–Al_2O_3, (c) Sn(3)–Al_2O_3, (d) Sn(5)–Al_2O_3 and (e) Sn(10)–Al_2O_3, (○) for γ-Al_2O_3.

Fourier transforms of the k^3-weighted EXAFS (extended X-ray absorption fine structure) spectra, phase-shift uncorrected, of Sn–Al_2O_3 along with that of pure SnO and SnO_2 are shown in Fig. 4B. Two distinct peaks ascribed to Sn–O (2.05 Å)[22] and Sn–Sn (3.71 Å)[22] bondings were observed in the Fourier transforms of the EXAFS spectrum of SnO_2. Obviously, the position of Sn–O bonding of all the Sn–Al_2O_3 samples was the same as that of pure SnO_2, while the second peak ascribed to Sn–Sn was not detected. These facts suggest the presence of finely-divided SnO_2 crystallites (abbreviated as "oxo-tin species") in the Sn–Al_2O_3 samples. The formation of "oxo-tin species" would be a feature of the sol–gel method employed here. Namely, an atomic-scale dispersion of Sn ions on the surface of fibrillar pseudo-boehmite sols with a length of 100 nm and a thickness of 10 nm[23,24] are expected in the dried gels, leading to the formation of Al–O–Sn bondings. Below 10 wt% Sn loading, tin oxides were estimated to be dispersed with a monolayer. Thus, the atomic-scale dispersion of Sn ions in the dried gels presumably resulted in the formation of tiny SnO_2 crystallites with a cluster size.

H_2-TPR experiments were carried out to clarify the nature of oxo-tin species. Figure 5 shows the TPR spectra of Sn–Al_2O_3 with different Sn loadings along with that of pure SnO_2. All of the Sn–Al_2O_3 samples, except for Sn(1)–Al_2O_3, which did not show any distinct H_2 consumption peaks below 1000 K, showed a similar TPR profile consisting of two well-resolved peaks centered at around 800 and 1100 K and a shoulder peak at ca. 600 K, although the amount of hydrogen uptake is different depending upon the Sn loading. The uptake of hydrogen molecules per Sn atoms is summarized in Table 2. For pure SnO_2, the H_2/Sn ratio is close to the stoichiometry for the reduction of bulk SnO_2 (H_2/Sn = 2), indicating that 98% of bulk SnO_2 can be reduced to Sn metal. As shown in Fig. 5, pure SnO_2 gave a sharp reduction peak centered at ca. 1060 K, indicating that the reduction of Sn^{IV} to Sn^0 may be kinetically fast at temperatures above 800 K. Interestingly, the H_2/Sn ratio for the reduction of Sn–Al_2O_3 was much smaller than the sto-

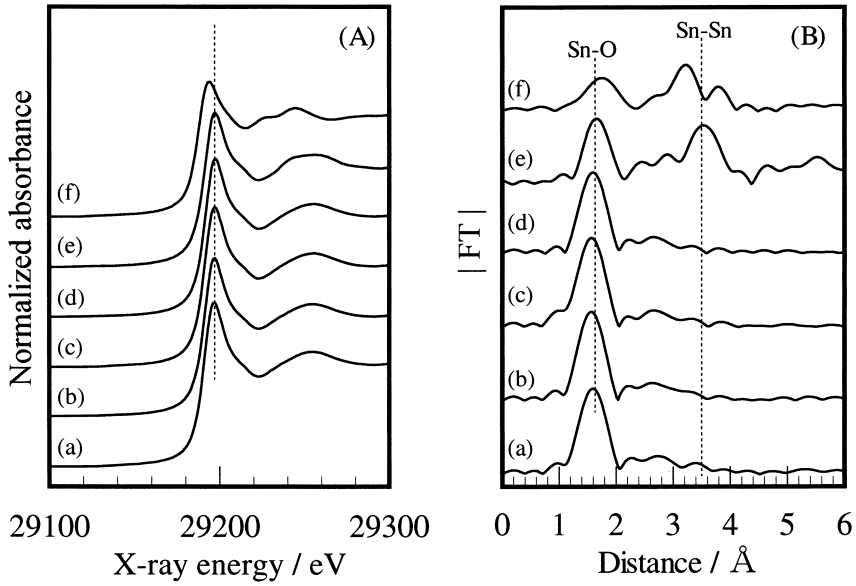

Fig. 4. (A) Sn K-edge XANES spectra and (B) Fourier transforms of EXAFS spectra of (a) Sn(1)–Al_2O_3, (b) Sn(3)–Al_2O_3, (c) Sn(5)–Al_2O_3, (d) Sn(10)–Al_2O_3, (e) SnO_2 and (f) SnO.

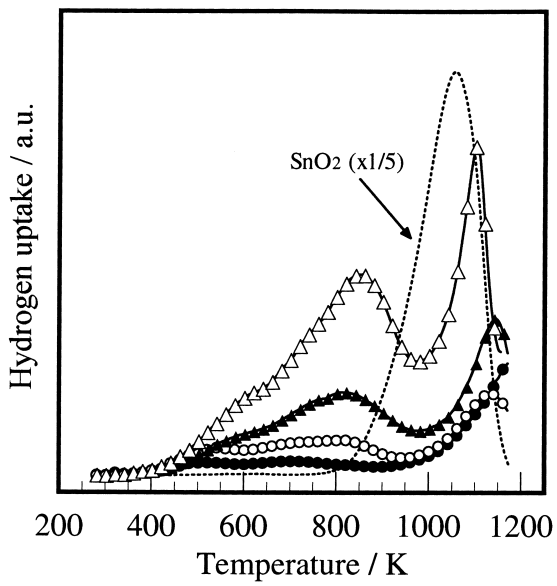

Fig. 5. TRP profiles of Sn–Al_2O_3 with different Sn loading and pure SnO_2.
(●) Sn(1)–Al_2O_3, (○) Sn(3)–Al_2O_3, (▲) Sn(5)–Al_2O_3, (△) Sn(10)–Al_2O_3, dotted line: SnO_2.

ichiometry (Table 2), whereas the reduction peak at around 1100 K was recognized in their TPR profiles. This is probably because some of oxo-tin species are incorporated into the bulk and strongly interacted with alumina, which is a characteristic of the sol–gel method.

The reduction peaks at around 570 and 850 K observed for Sn–Al_2O_3 can be ascribed to a reduction of the surface vicinity of oxo-tin species and the reduction of Sn^{IV} to Sn^{II}, respectively.[16,18] Auroux et al.[18] reported that easily reducible Sn^{IV} species to Sn^{II} species is an active phase for lean NO_x catalysis. Thus, the ratio of the surface vicinity reduced below 973 K to the total oxo-tin species reduced below 1173 K ($Sn_{(IV\rightarrow II)}/Sn_{(total)}$) was calculated. As given in Table 2, no correlation between the catalytic activity and the $Sn_{(IV\rightarrow II)}/Sn_{(total)}$ ratio was observed. This is probably because not only oxo-tin species, but also alumina, participate in the reaction as catalytically active sites.

Table 2. Summary of TPR Measurements

Catalyst	mol H_2/mol Sn[a)]	% H_2 consumption below 973 K ($Sn_{(IV\rightarrow II)}/Sn_{(total)}$)
SnO_2	1.98	0.50[b)]
Sn(1)–Al_2O_3	0.77	33.8
Sn(3)–Al_2O_3	0.80	56.3
Sn(5)–Al_2O_3	0.75	58.6
Sn(10)–Al_2O_3	0.75	64.2

a) H_2 uptake detected below 1173 K was divided by the total Sn content.
b) The ratio of H_2 uptake below 673 K to that below 1173 K.

3. Effect of H_2O Treatment. Kung et al.[15,16] reported that the catalytic activity of Sn/Al_2O_3 was improved by 5–20% after a pretreatment in the reaction gases (NO + C_3H_6 + O_2 + H_2O) at 873 K, although they have not revealed the reasons. It was also reported that the presence of H_2O considerably enhanced the activity of tin-containing catalysts, such as Sn–ZSM-5 + MnO_2[25] and SnO_2–Ga_2O_3–Al_2O_3,[26] for NO reduction. These reports indicate that coexisting H_2O often affects the catalytic performance of tin-containing catalysts. Accordingly, the catalytic activity of Sn–Al_2O_3 for NO reduction in the absence of H_2O was evaluated before and after an H_2O treatment in flowing 9.1% H_2O/He at 873 K for 3 h. The results are shown in Fig. 6. It appears that the catalytic activity of Al_2O_3 was not affected by the H_2O treatment at all. On the contrary, the H_2O treatment caused an enhancement of the NO reduction activity of Sn–Al_2O_3 in the entire temperature range

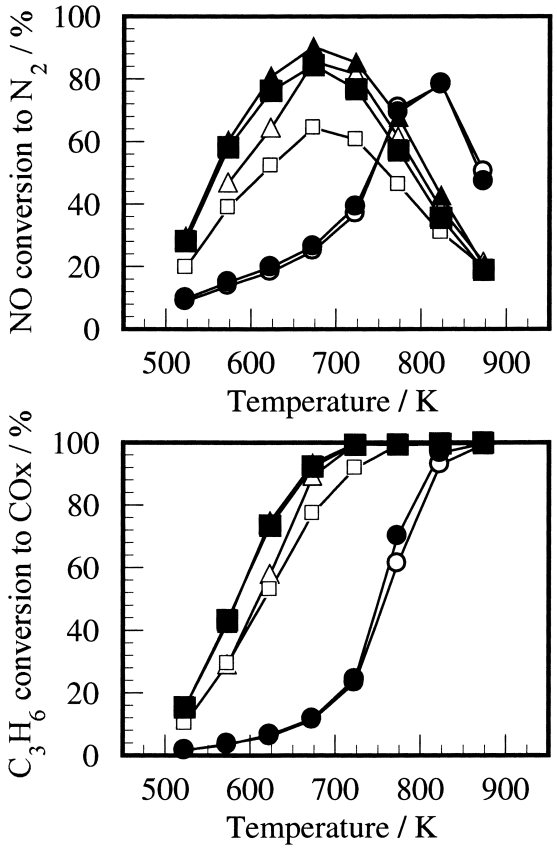

Fig. 6. Effect of H_2O treatment on the catalytic activity of Al_2O_3 (○,●), Sn(5)–Al_2O_3 (△,▲) and Sn(10)–Al_2O_3 (□,■) for NO reduction by propene in the absence of H_2O. Conditions: NO = 880 ppm, C_3H_6 = 950 ppm, O_2 = 9.3%, H_2O = 0%, W/F = 0.18 gs cm^{-3}. Open symbols (○,△,□) are the results of fresh catalysts and closed ones (●,▲,■) are of H_2O-treated catalysts.

irrespective of Sn loading. Particularly, a remarkable activity enhancement was observed for Sn(10)–Al_2O_3. Since C_3H_6 conversion was also increased, H_2O treatment may alter the Sn species as catalytically active sites.

The physical properties of the H_2O-treated Sn–Al_2O_3 are summarized in Table 3. It can be seen by comparing Tables 1 and 3 that the H_2O treatment did not change the BET surface area of Sn–Al_2O_3, but decreased the concentration of Cl^- ions by about 30%. This suggests that tin chloride remaining after the calcination at 873 K may be hydrolyzed to tin oxide during the H_2O treatment. The fact that no great difference in the XRD spectra was observed between the fresh and the H_2O-treated Sn–Al_2O_3 (results not shown) indicates that the H_2O treatment does not affect the crystal structure of the catalysts and the dispersion state of the Sn species.

Figure 7 shows the TPR profiles of the fresh and the H_2O-treated Sn–Al_2O_3. It appears that the H_2/Sn ratio calculated from the total H_2 uptake below 1173 K was increased by the H_2O treatment (Table 3), meaning an increase of reducible oxo-tin species. From these results, the activity enhancement caused by the H_2O treatment can be attributed to the following two reasons: (i) increase of the surface concentration of oxo-tin species and (ii) modification of oxo-tin species as active

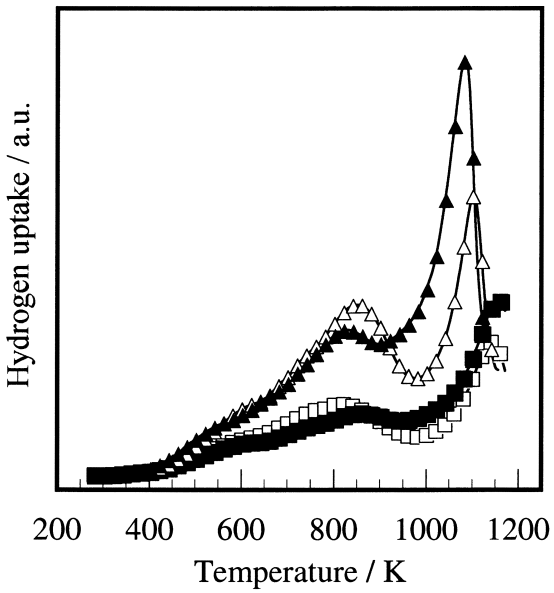

Fig. 7. Effect of H_2O treatment on the TPR profiles of Sn(5)–Al_2O_3 (□,■) and Sn(10)–Al_2O_3 (△,▲). Open symbols (□,△) are the results of fresh catalysts and closed ones (■,▲) are of H_2O-treated catalysts.

sites accompanied by the removal of Cl^- ions.

4. Kinetic Studies of NO Reduction by Propene over Sn–Al_2O_3. The kinetic parameters and the activation energies for N_2 and CO_x formation over fresh and H_2O-treated Sn(5)–Al_2O_3 are summarized in Table 4, where the former was determined from ln–ln plots of the rate against the partial pressure of NO, C_3H_6 or O_2 and the latter from the Arhenius plots. A good linear correlation was observed within the experimental errors. As given in Table 4, the activation energy for N_2 and CO_x formation decreased by about 70% after H_2O treatment. This may be due to the modification of the catalytically active sites described above. However, a significant difference in the reaction orders with respect to NO, C_3H_6 and O_2 for N_2 and CO_x formation was not observed between the fresh and the H_2O-treated catalysts. This leads us to deduce that the H_2O treatment does not affect the reaction steps for activation of the reaction gases.

As can be seen in Table 4, the reaction order with respect to NO for N_2 formation was less than unity, indicating the presence of NO_x adspecies on the catalyst surface, mainly on Al_2O_3. In agreement with the literature,[27–29] NO_x adspecies may behave as an intermediate for N_2 formation. The formation of NO_x adspecies by the reaction of NO + O_2 was evidenced by NO_x-TPD measurements (results not shown). On the other hand, NO_x adspecies seem to inhibit C_3H_6 oxidation to intermediates (abbreviated as C_3H_6-derived species) and/or CO_x, because the reaction order with respect to NO for CO_x formation was −0.3 (Table 4). Probably, NO_x adspecies and C_3H_6-derived species compete on the same adsorption sites.

Recently, we conducted kinetic studies for NO reduction by propene over Al_2O_3 to determine the kinetic parameters, and found that the reaction orders with respect to NO, C_3H_6, and O_2 for N_2 formation were 0.3, 0.3, and 0.6, respectively.[30] Apparently, the reaction orders on Al_2O_3 are almost the same as

Table 3. Characteristics of H_2O-Treated Sn–Al_2O_3[a)]

Catalyst	BET surface area/$m^2\ g^{-1}$	Elemental analysis		TPR[c)]
		Sn/Al[b)]	Cl/Al	mol H_2/mol Sn
Al_2O_3	154	na	na	na
Sn(5)–Al_2O_3	221	0.021 (0.023[b)])	0.003	0.80
Sn(10)–Al_2O_3	248	na	na	0.85

a) Conditions for H_2O treatment: H_2O = 9.1%, temperature = 873 K, treatment time = 3 h.
b) In parentheses are given calculated atomic ratio.
c) TPR profiles are shown in Fig. 7.

Table 4. Kinetic Parameters of the Selective Reduction of NO with Propene over Sn(5)–Al_2O_3 at 623 K

Catalyst	Product	Reaction order[a)] with respect to			Activation energy[b)]
		NO	C_3H_6	O_2	/kJ mol^{-1}
Fresh Sn(5)–Al_2O_3	N_2	0.3	0.4	0.7	43
	CO_x	−0.3	0.7	0.7	49
H_2O-treated Sn(5)–Al_2O_3	N_2	0.2	0.5	0.8	30
	CO_x	−0.3	0.8	0.5	35

a) Conditions: NO = 180–1500 ppm, C_3H_6 = 150–1900 ppm, O_2 = 2–15%, temperature = 623 K, gas flow rate = 66 $cm^3\ min^{-1}$, catalyst weight = 0.03–0.1 g.
b) Activation energies were calculated by varing the temperatures from 623 to 723 K under the following reaction conditions: NO = 880 ppm, C_3H_6 = 950 ppm, O_2 = 9.3%, H_2O = 0%, gas flow rate = 66 $cm^3\ min^{-1}$.

those on Sn–Al_2O_3. On the other hand, the addition of SnO_2 into Al_2O_3 caused a decrease in the activation energy for N_2 formation, from 85 to 43 kJ mol^{-1}. These results suggest that the supported-SnO_2 promotes important reaction steps for N_2 formation on Al_2O_3 sites. A similar bifunctional effect of SnO_2 and Al_2O_3 has been reported by Yezerets et al.[31] They revealed that SnO_2 promotes the activation of C_3H_6 to form oxygenated intermediates, which subsequently react with NO_x on Al_2O_3 to yield N_2. In the present work, the role of supported-SnO_2 may be to activate C_3H_6 to intermediates, because the conversion of C_3H_6 on Sn–Al_2O_3 was similar to that on SnO_2, but much higher than that on Al_2O_3 (Figs. 1 and 2). The subsequent reactions of C_3H_6-derived intermediates and NO_x adspecies, leading to the formation of N_2, would proceed on Al_2O_3.

Conclusions

The following conclusions were obtained in the present work:

(1)Sn–Al_2O_3 prepared by the sol–gel method exhibited high catalytic activity for NO reduction by propene, compared with Al_2O_3 and SnO_2. The maximum NO conversion did not change much in the range of Sn loading of 1 and 5 wt%.

(2)Structural characterizations confirmed the presence of finely dispersed SnO_2 crystallites. Not only the surface of suppored-SnO_2, but also Al_2O_3, were suggested to behave as active sites. The role of suppored-SnO_2 was considered to activate C_3H_6 to intermediates, the subsequent reaction steps leading to N_2 formation to proceed on Al_2O_3.

(3)An H_2O treatment of Sn–Al_2O_3 caused a remarkable enhancement of the NO reduction activity. This promotional effect was interpreted by an increase of the surface SnO_2 concentration and a modification of the oxo-tin species as catalytically active sites, but not by a change of the reaction pathway.

We would like to express our sincere thanks to Mr. Kazuhito Sato of Cosmo Research Institute for his assistance in ICP analysis.

References

1 M. Shelef, *Chem. Rev.*, **95**, 209 (1995).
2 M. Iwamoto, H. Yahiro, S. Shundo, Y. Yu-u, and N. Mizuno, *Appl. Catal.*, **69**, L15 (1991).
3 W. Held, A. Koenig, T. Richter, and L. Puppe, *SAE Paper*, **1990**, 900496.
4 Ger. Offen. DE 3,642,018 (1987) to Volkswagen A.G.
5 Ger. Offen. DE 3,735,151 (1988) to Toyota Co.
6 C. Yokoyama and M. Misono, *J. Catal.*, **150**, 9 (1994).
7 Y. Li and J. N. Armor, *Appl. Catal. B*, **2**, 239 (1993).
8 E. Kikuchi and K. Yogo, *Catal. Today*, **22**, 73 (1996).
9 R. A. Grinstedt, H.-W. Jen, C. N. Montreuil, M. J. Rokosz, and M. Shelef, *Zeolites*, **13**, 602 (1993).
10 H. Hamada, *Catal. Today*, **22**, 21 (1994).
11 M. C. Kung and H. H. Kung, *Top. Catal.*, **10**, 21 (2000).
12 Y. Kintaichi, H. Hamada, M. Tabata, M. Sasaki, and T. Ito, *Catal. Lett.*, **6**, 239 (1990).
13 Y. Teraoka, T. Harada, T. Iwasaki, T. Ikeda, and S. Kagawa, *Chem. Lett.*, **1993**, 773.
14 M. Tabata, H. Hamada, F. Suganuma, T. Yoshinari, H. Tsuchida, Y. Kintaichi, M. Sasaki, and T. Ito, *Catal. Lett.*, **25**, 55 (1994).
15 M. C. Kung, P. W. Park, D.-W. Kim, and H. H. Kung, *J. Catal.*, **181**, 1 (1999).
16 P. W. Park, H. H. Kung, D.-W. Kim, and M. C. Kung, *J. Catal.*, **184**, 440 (1999).
17 J. Ma, Y. Zhu, J. Wei, X. Cai, and Y. Xie, *Stud. Surf. Sci. Catal.*, **130**, 617 (2000).
18 A. Auroux, D. Sprinceana, and A. Gervasini, *J. Catal.*, **195**,

140 (2000).

19 A. Ueno, H. Suzuki, and Y. Kotera, *J. Chem. Soc., Faraday Trans. 1*, **79**, 127 (1983).

20 M. Haneda, T. Mizushima, B. Kakuta, A. Ueno, Y. Sato, S. Matsuura, K. Kasahara, and M. Sato, *Bull. Chem. Soc. Jpn.*, **66**, 1279 (1993).

21 Y. Kintaichi, M. Haneda, M. Inaba, and H. Hamada, *Catal. Lett.*, **48**, 121 (1997).

22 A. A. Bolzan, C. Fong, B. J. Kennedy, and C. J. Howard, *Acta Crystallogr.*, **B53**, 373 (1997).

23 K. Ishiguro, T. Ishikawa, N. Kakuta, A. Ueno, Y. Mitarai, and T. Kamo, *J. Catal.*, **123**, 523 (1990).

24 T. Ishikawa, R. Ohashi, H. Nakabayashi, N. Kakuta, A. Ueno, and A. Furuta, *J. Catal.*, **134**, 87 (1992).

25 Y. Hirao, C. Yokoyama, and M. Misono, *J. Chem. Soc, Chem. Commun.*, **1996**, 597.

26 M. Haneda, Y. Kintaichi, and H. Hamada, *Appl. Catal. B*, **20**, 289 (1999).

27 S. Kameoka, Y. Ukisu, and T. Miyadera, *Phys. Chem. Chme. Phys.*, **2**, 367 (2000).

28 F. C. Meunier, J. P. Breen, V. Zuzaniuk, M. Olsson, and J. R. H. Ross, *J. Catal.*, **187**, 493 (1999).

29 K. Shimizu, H. Kawabata, A. Satsuma, and T. Hattori, *J. Phys. Chem. B*, **103**, 5240 (1999).

30 M. Haneda, Y. Kintaichi, H. Shimada, and H. Hamada, *J. Catal.*, **192**, 137 (2000).

31 A. Yezerets, Y. Zheng, P. W. Park, M. C. Kung, and H. H. Kung, *Stud. Surf. Sci. Catal.*, **130**, 629 (2000).